Classical Simulation of Relativistic *Zitterbewegung* in Photonic Lattices

Felix Dreisow,[1] Matthias Heinrich,[1] Robert Keil,[1] Andreas Tünnermann,[1] Stefan Nolte,[1] Stefano Longhi,[2] and Alexander Szameit[1,3,*]

[1]*Institute of Applied Physics, Friedrich-Schiller-Universität, Max-Wien-Platz 1, 07743 Jena, Germany*
[2]*Dipartimento di Fisica, Politecnico di Milano, Piazza Leonardo da Vinci 32, 20133 Milan, Italy*
[3]*Physics Department and Solid State Institute, Technion, 32000 Haifa, Israel*
(Received 23 July 2010; revised manuscript received 27 August 2010; published 28 September 2010)

We present the first experimental realization of an optical analog for relativistic quantum mechanics by simulating the *Zitterbewegung* (trembling motion) of a free Dirac electron in an optical superlattice. Our photonic setting enables a direct visualization of *Zitterbewegung* as a spatial oscillatory motion of an optical beam. Direct measurements of the wave packet expectation values in superlattices with tuned miniband gaps clearly show the transition from weak-relativistic to relativistic and far-relativistic regimes.

DOI: 10.1103/PhysRevLett.105.143902 PACS numbers: 42.82.Et, 03.65.Pm

Simulating the evolution of a nonrelativistic quantum-mechanical particle in a periodic potential by propagating an optical wave packet in arrays of evanescently coupled waveguides has received continuous and increasing attention in recent years [1]. The underlying idea of mapping nonrelativistic quantum mechanics onto an optical model system is the conceptual similarity between the Schrödinger equation for matter waves and the scalar paraxial wave equation for optical waves. This formal correspondence allowed for the observation of various classical analogues of nonrelativistic phenomena commonly associated with the evolution of electrons in periodic potentials, such as optical Bloch oscillations [2] and Zener tunneling [3], optical dynamic localization [4], Anderson localization in disordered lattices [5], and geometric potentials in topological crystals [6]. It is a common belief that the use of optical waveguides as a model system for quantum mechanics carries the intrinsic drawback of being limited to nonrelativistic phenomena and that the observation of optical analogues of relativistic phenomena requires subwavelength structured media like photonic crystals or metamaterials [7–9]. However, only recently it has been realized that, by carefully designing the underlying periodic potential, paraxial light propagation is capable of simulating the evolution of a relativistic quantum particle, as described by the spinor-type Dirac equation. Thus, optical analogues of such important phenomena as Klein tunneling [10,11] and *Zitterbewegung* (ZB) [12] can be realized in the framework of paraxial optics in periodic media, without requiring specially synthesized media with subwavelength controlled properties.

The concept of ZB was first introduced by Schrödinger when analyzing the properties of Dirac's relativistic wave equation [13]. He found that a free relativistic electron exhibits a rapid trembling motion due to interference between positive and negative energy states [14]. The phenomenon of ZB raised a lively and controversial debate since it was unclear how an intrinsic single-particle equation as the Dirac equation can describe a multiparticle phenomenon as ZB, where at least two particles (the electron and its counterpart in the Dirac sea, the positron) are required [15]. A direct experimental confirmation of ZB for relativistic electrons is very unlikely, mainly because of the extremely small amplitude of the trembling motion (of the order of the Compton wavelength $\approx 10^{-12}$ m) and the extremely high oscillation frequency ($\approx 10^{21}$ Hz). Various analogous systems were suggested in order to observe this effect, such as tight-binding semiconductor lattice models [16], trapped ions [17], graphene [18], ultracold neutral atoms [19], and—in photonic settings—two-dimensional photonic crystals [8] and negative-zero-positive index metamaterials [9]. The search for experimentally accessible systems that are described by a Dirac-type equation has received a great amount of attention in the past few years, culminating in the recent demonstration of a quantum simulator of the Dirac equation and the observation of ZB using a single trapped ion set to behave as a free relativistic quantum particle [20].

In this Letter we present a classical simulator of the relativistic Dirac equation in an optical setting, with the observation of ZB for optical beams. We demonstrate that the two-component (spinor) wave function dynamics of the Dirac equation can be simulated by paraxial light propagation in an optical superlattice, where the spinor is represented by the two lattice sites within the primitive unit cell. Our photonic setting enables a direct visualization of ZB as a spatial oscillatory motion of an optical beam in the superlattice and allows us to observe the transition from the far- to the weak-relativistic regime by tuning the gap between the two superlattice minibands [16].

The optical structures realized for our experiments consist of a set of 75 mm-long binary waveguide arrays composed by two interleaved sublattices *A* and *B* [Fig. 1(a)] manufactured in fused silica samples using the laser-direct writing technology [21]. The two sublattices are realized by writing an alternating sequence of waveguides with high and low index change separated by the same distance

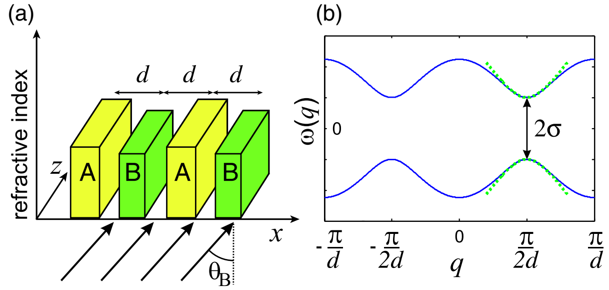

FIG. 1 (color online). (a) Refractive index profile of the binary waveguide system consisting of an alternating sequence of high (A) and low (B) index waveguides; the arrows show beam excitation in real space under the Bragg angle θ_B. (b) Band structure of the binary array, comprising two minibands separated by 2σ. The dotted curve shows the hyperbolic dispersion curve of the Dirac equation near $q = \pi/(2d)$.

a [22]. As noticed in [12], spatial propagation of a monochromatic paraxial light field $E(x, z)$ (x and z are the transverse and longitudinal coordinates, respectively) at wavelength λ along the waveguides simulates the free motion of a relativistic massive particle in one spatial dimension whenever the lattice excitation is accomplished by a broad beam tilted near the Bragg angle. In the tight-binding approximation, the field $E(x, z)$ can be expanded into a superposition of confined modes trapped in the various guides, and light transport is described by the coupled-mode equations [23]

$$i\frac{da_n}{dz} = -\kappa(a_{n+1} + a_{n-1}) + (-1)^n \sigma a_n, \quad (1)$$

where a_n are the modal field amplitudes in the various waveguides and 2σ and κ are the propagation constant mismatch and the coupling rate between two adjacent waveguides of the array, respectively. The superlattice supports two minibands, separated by a narrow gap of width 2σ [see Fig. 1(b)], defined by the dispersion curves [22] $\omega_\pm(q) = \pm\sqrt{\sigma^2 + 4\kappa^2\cos^2(qd)}$, where $2d$ is the lattice period and q the Bloch wave number. Hence, in the vicinity of the edges of the first Brillouin zone, e.g., near $q = \pi/(2d)$, the dispersion curves of the two minibands form two opposite hyperbolas, and therefore mimic the typical hyperbolic energy-momentum dispersion relation for positive-energy and negative-energy branches of a freely moving relativistic massive particle (dotted graph). This suggests that light transport in the lattice for Bloch waves with wave number q close to $\pi/(2d)$ simulates the temporal dynamics of the relativistic Dirac equation. When launching a broad beam tilted at the Bragg angle $\theta_B \simeq \lambda/(4n_s d)$ (n_s is the substrate refractive index) into the array, only a small region around $q = \pi/(2d)$ in q space is excited. After setting $a_{2n}(z) = (-1)^n \psi_1(n, z)$ and $a_{2n-1} = -i(-1)^n \psi_2(n, z)$ and introducing the continuous transverse coordinate $\xi \leftrightarrow n = x/(2d)$, the two-component spinor $\psi(\xi, z) = (\psi_1, \psi_2)^T$ satisfies the one-dimensional Dirac equation [12,16]

$$i\frac{\partial\psi}{\partial z} = -i\kappa\alpha\frac{\partial\psi}{\partial\xi} + \sigma\beta\psi, \quad (2)$$

where

$$\alpha = \begin{pmatrix} 0 & 1 \\ 1 & 0 \end{pmatrix} \quad \text{and} \quad \beta = \begin{pmatrix} 1 & 0 \\ 0 & -1 \end{pmatrix}$$

are the σ_x and σ_z Pauli matrices, respectively. Equation (2) corresponds to the one-dimensional Dirac equation for a relativistic freely moving particle of mass m provided that the formal change,

$$\kappa \to c, \qquad \sigma \to mc^2/\hbar, \quad (3)$$

is made, and ξ and z are interpreted as the spatial and the temporal variables, respectively. Therefore, in our optical setting the temporal evolution of the Dirac spinor wave function ψ is mapped onto the spatial evolution along z of the field amplitudes ψ_1 and ψ_2, describing the occupation amplitudes of light in the two sublattices A and B of the binary array. Correspondingly, ZB is observed as a quivering spatial oscillatory motion of the beam center of mass $\langle n\rangle(z) = \sum_n n|a_n|^2/\sum_n|a_n|^2$. Note that the measurable quantity $\langle n\rangle(z)$ is directly related to the expectation value of position for the relativistic particle, $\langle\xi\rangle(z) = [\int d\xi\xi(|\psi_1|^2 + |\psi_2|^2)]/[\int d\xi(|\psi_1|^2 + |\psi_2|^2)]$, by the simple relation $\langle n\rangle \simeq 2\langle\xi\rangle + 1/2$ [12]. When the envelope G for the initial light field $E(x, 0) = G(x) \times \exp(2\pi i x n_s\theta_B/\lambda)$, which is tilted at the Bragg angle θ_B, varies slowly over the waveguide spacing d, an exact expression for $\langle\xi\rangle(z)$ can be derived and reads [12]

$$\langle\xi\rangle(z) = \langle\xi\rangle(0) + v_0 z + 2\pi\kappa\sigma^2\int dk(1/\epsilon^3) \times \sin(2\epsilon z)|\hat{G}(k)|^2, \quad (4)$$

where $k = 2qd - \pi$ is the shifted transverse momentum, $\epsilon(k) = \sqrt{\sigma^2 + \kappa^2k^2}$ defines the energy-momentum dispersion relation of the free relativistic particle, $\hat{G}(k) = (1/2\pi)\int d\xi G(2d\xi)\exp(-ik\xi)$ is the angular spectrum of the beam envelope, and $v_0 = 4\pi\kappa^3\int dk(k/\epsilon)^2|\hat{G}(k)|^2$ is the mean particle speed [24]. The last oscillatory term on the right-hand side of Eq. (4), superimposed to the straight trajectory defined by the first two terms, is the ZB. For $\hat{G}(k)$ centered at $k = 0$, at leading order Eq. (4) yields $\langle\xi\rangle \times (z) \simeq \langle\xi\rangle(0) + v_0 z + (\kappa/2\sigma)\sin(2\sigma z)$; i.e., the amplitude and frequency of ZB are given by

$$R_{\rm ZB} = \kappa/(2\sigma) = \hbar/(2mc), \quad (5)$$

$$\omega_{\rm ZB} = 2\sigma = 2mc^2/\hbar, \quad (6)$$

respectively [25]. Therefore, ZB vanishes for either the far-relativistic ($m \to 0$) or the weak-relativistic ($m \to \infty$) limits: in the first case the amplitude of ZB diverges, but the oscillation frequency $\omega_{\rm ZB}$ goes to zero, whereas in the latter case the frequency of ZB diverges, but its amplitude vanishes (see, for instance, [16]).

In our experiments, the transition between the different regimes is realized by tuning the propagation constant mismatch σ, keeping the coupling rate κ of adjacent waveguides constant ($\kappa = 0.14\ \text{mm}^{-1}$ for a waveguide spacing $d = 16\ \mu\text{m}$). The tuning of σ is accomplished by varying the ratio between the writing velocities of adjacent waveguides in the sublattices A and B. A fluorescence microscopy technique [26] enables us to map the flow of light from the top of the sample, and thus to visualize the spinor wave packet evolution.

The first superlattice was designed and manufactured to approach the far-relativistic regime ($\sigma = 0.07\ \text{mm}^{-1} = 0.5\kappa$). This corresponds to a small particle mass [see Eq. (3)] and therefore a large ZB period $\Lambda_{\text{ZB}} = 2\pi/\omega_{\text{ZB}} = \pi/\sigma$ accompanied by a large ZB amplitude R_{ZB}, according to Eqs. (5) and (6). The array was excited by a broad Gaussian beam at a wavelength of $\lambda = 633$ nm with a spot size of $\simeq 105\ \mu$m in the horizontal x direction, covering approximately 7 waveguides. The Bragg angle of $\theta_B \simeq 0.39°$ was carefully aligned by mounting the sample onto a precision rotation stage. As calibration we used a homogeneous waveguide array, where we adjusted the propagating beam to minimal diffraction, which exactly occurs at the Bragg angle [27]. The fluorescence image of the beam propagation inside the sample, simulating the far-relativistic regime, is shown in Fig. 2(a). The results are compared to numerical simulations [Fig. 2(a)], based on the coupled-mode equations [Eq. (1)]. One clearly sees an oscillation of the beam, accompanied by a transverse drift. The oscillations turn out to be asymmetric, a feature which is ascribable to the angular spectral broadening of the launching beam. The ZB is clearly observed when the beam center of mass $\langle n\rangle(z)$ is extracted from the fluorescence image. The result, depicted in Fig. 2(c), shows that beam oscillations around the straight mean path occur with a ZB amplitude of 1 waveguide (16 μm) and with a large period of $\Lambda_{\text{ZB}} = 44.9$ mm, in good agreement with the theoretical predictions. Owing to the limited length of the sample, only two beam oscillations are visible for the chosen small value of the mismatch σ.

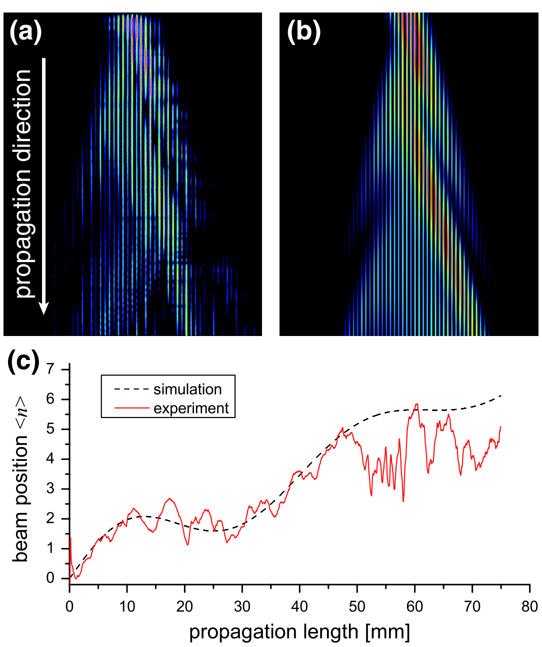

FIG. 2 (color online). Far-relativistic regime of ZB for $\sigma = 0.5\kappa$. (a) Measured light distribution along the sample and (b) corresponding numerical simulation. (c) Measured (solid line) and calculated (dashed line) path of the beam center of mass $\langle n\rangle(z)$.

As σ is increased to reach the same order as κ, the relativistic regime, corresponding to a moderate ZB amplitude and to a shorter ZB period, is attained. As an example, Fig. 3 shows the experimental measurements, together with the theoretical predictions, of beam propagation and ZB in a binary array with a mismatch of $\sigma = 0.15\ \text{mm}^{-1} = 1.1\kappa$. The beam clearly exhibits a pronounced trembling motion around the main trajectory, with a shorter ZB period ($\Lambda_{\text{ZB}} = 20.4$ mm) but smaller ZB amplitude (0.45 waveguides $= 7\ \mu$m) as compared to the case of Fig. 2. Note also that, as compared to Fig. 2, the transverse beam drift is greatly reduced. This is due to the fact that the drift velocity v_0 decreases as the ratio σ/κ increases.

By further increasing the propagation constant mismatch, the weak-relativistic regime, corresponding to a very rapid trembling motion but with almost vanishing amplitude, can be observed. As an example, Fig. 4 shows the experimental measurements and numerical simulations for a binary array with $\sigma = 0.3\ \text{mm}^{-1} = 2.1\kappa$. In this case, from Fig. 4(c) the oscillation period and ZB amplitude turn out to be $\Lambda_{\text{ZB}} = 10.7$ mm and 0.25 waveguides ($=4\ \mu$m), respectively. Note that the diminishing of both ZB period and ZB amplitude is also accompanied by a lowering of the transverse beam drift, i.e., of v_0. By further increasing the mismatch σ, beam oscillations get basically too small to be measured, entering in the nonrelativistic regime.

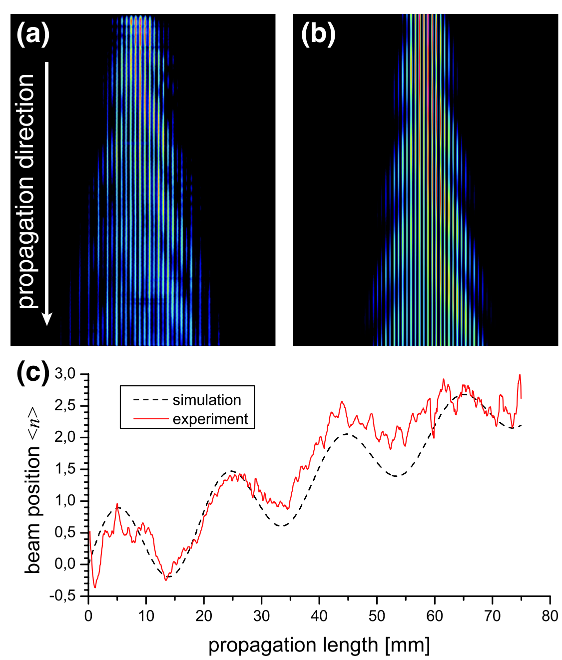

FIG. 3 (color online). Same as Fig. 2, but for $\sigma = 1.1\kappa$.

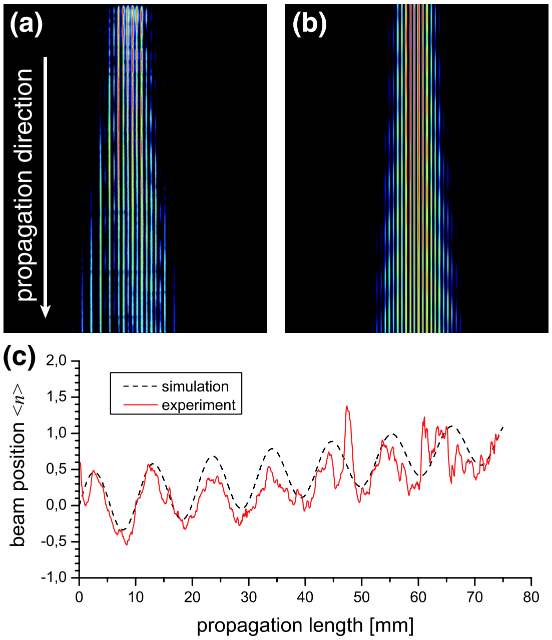

FIG. 4 (color online). Same as Fig. 2, but for $\sigma = 2.1\kappa$.

In conclusion, we reported on the first experimental realization of a classical simulator of relativistic quantum mechanics, with the observation of an optical analogue of relativistic *Zitterbewegung*. Our results suggest that waveguide optics could provide an experimentally accessible classical simulator to test other relativistic effects rooted in the Dirac equation, such as the dynamical process of pair production or Rabi oscillations of the Dirac sea [28]. In future experiments the femtosecond laser waveguide writing technique can be employed to realize the above mentioned and further relativistic effects. As compared to other classical or quantum simulators of the Dirac equation [8,9,20], our photonic setting enables a direct visualization of the spinor wave function evolution, without requiring the synthesis of special optical media with subwavelength controlled properties nor complex or indirect imaging techniques. On the other hand, optical waveguide arrays are only limited by the resolution of the setup, which is advantageous for the simulation of larger, in particular, two-dimensional systems, where numerical simulators also reach computational limits.

The authors acknowledge support by the Deutsche Forschungsgemeinschaft (Research Unit 532 and Leibniz program), the German Academy of Science Leopoldina (Grant No. LPDS 2009-13), and the Italian MIUR (PRIN 2008 project "Analogie ottico-quantistiche in strutture fotoniche a guida d'onda").

*alexander.szameit@uni-jena.de

[1] S. Longhi, Laser Photon. Rev. **3**, 243 (2009).
[2] T. Pertsch *et al.*, Phys. Rev. Lett. **83**, 4752 (1999); R. Morandotti *et al.*, Phys. Rev. Lett. **83**, 4756 (1999).
[3] M. Ghulinyan *et al.*, Phys. Rev. Lett. **94**, 127401 (2005); H. Trompeter *et al.*, Phys. Rev. Lett. **96**, 023901 (2006).
[4] S. Longhi *et al.*, Phys. Rev. Lett. **96**, 243901 (2006).
[5] T. Schwartz *et al.*, Nature (London) **446**, 52 (2007); Y. Lahini *et al.*, Phys. Rev. Lett. **100**, 013906 (2008).
[6] A. Szameit, F. Dreisow, M. Heinrich, R. Keil, S. Nolte, A. Tünnermann, and S. Longhi, Phys. Rev. Lett. **104**, 150403 (2010).
[7] F. D. M. Haldane and S. Raghu, Phys. Rev. Lett. **100**, 013904 (2008); R. A. Sepkhanov, Ya. B. Bazaliy, and C. W. J. Beenakker, Phys. Rev. A **75**, 063813 (2007); O. Peleg, G. Bartal, B. Freedman, O. Manela, M. Segev, and D. N. Christodoulides, Phys. Rev. Lett. **98**, 103901 (2007); O. Bahat-Treidel, O. Peleg, and M. Segev, Opt. Lett. **33**, 2251 (2008).
[8] X. Zhang, Phys. Rev. Lett. **100**, 113903 (2008).
[9] L. G. Wang, Z. G. Wang, J. X. Zhang, and S. Y. Zhu, Opt. Lett. **34**, 1510 (2009).
[10] O. Bahat-Treidel, O. Peleg, M. Grobman, N. Shapira, M. Segev, and T. Pereg-Barnea, Phys. Rev. Lett. **104**, 063901 (2010).
[11] S. Longhi, Phys. Rev. B **81**, 075102 (2010).
[12] S. Longhi, Opt. Lett. **35**, 235 (2010).
[13] E. Schrödinger, Sitzungsber. Preuss. Akad. Wiss. Phys. Math. Kl. **24**, 418 (1930).
[14] K. Huang, Am. J. Phys. **20**, 479 (1952).
[15] P. Krekora, Q. Su, and R. Grobe, Phys. Rev. Lett. **93**, 043004 (2004); Z. Y. Wang and C. D. Xiong, Phys. Rev. A **77**, 045402 (2008).
[16] F. Cannata, L. Ferrari, and G. Russo, Solid State Commun. **74**, 309 (1990).
[17] L. Lamata, J. Leon, T. Schätz, and E. Solano, Phys. Rev. Lett. **98**, 253005 (2007).
[18] J. Cserti and G. David, Phys. Rev. B **74**, 172305 (2006); T. M. Rusin and W. Zawadzki, Phys. Rev. B **76**, 195439 (2007).
[19] J. Y. Vaishnav and C. W. Clark, Phys. Rev. Lett. **100**, 153002 (2008).
[20] R. Gerritsma, G. Kirchmair, F. Zähringer, E. Solano, R. Blatt, and C. F. Roos, Nature (London) **463**, 68 (2010).
[21] K. Davies, K. Miura, N. Sugimoto, and K. Hirao, Opt. Lett. **21**, 1729 (1996); K. Itoh, W. Watanabe, S. Nolte, and C. B. Schaffer, MRS Bull. **31**, 620 (2006).
[22] F. Dreisow, A. Szameit, M. Heinrich, T. Pertsch, S. Nolte, A. Tünnermann, and S. Longhi, Phys. Rev. Lett. **102**, 076802 (2009).
[23] A. A. Sukhorukov and Y. S. Kivshar, Opt. Lett. **27**, 2112 (2002).
[24] In writing Eq. (4), the normalization condition $\int dk|\hat{G}(k)|^2 = 1/(4\pi)$ has been used.
[25] The broadening of the angular spectrum $\hat{G}(k)$ is responsible for the damping of ZB.
[26] A. Szameit, F. Dreisow, H. Hartung, S. Nolte, and A. Tünnermann, Appl. Phys. Lett. **90**, 241113 (2007); F. Dreisow, M. Ornigotti, A. Szameit, M. Heinrich, R. Keil, S. Nolte, A. Tünnermann, and S. Longhi, Appl. Phys. Lett. **95**, 261102 (2009).
[27] H. S. Eisenberg, Y. Silberberg, R. Morandotti, and J. S. Aitchison, Phys. Rev. Lett. **85**, 1863 (2000).
[28] S. Longhi, Phys. Rev. A **81**, 022118 (2010).